Compatibility of high-Z impurity accumulation with high plasma performance in ECR-heated W7-X plasmas

D. Zhang, M.N.A. Beurskens, J.A Alcusón[1], G. Wurden[2], B. Buttenschön, S. Jablonski[3] , M. Kubkowska[3], A. Langenberg, K. Rahbarnia, F. Reimold, A. Pavone, S. Kwak, H. M. Smith, C.D. Beidler, S.A. Bozhenkov, O. Ford, C. Biedermann, K.J. Brunner, R. Burhenn, Y. Feng, G. Fuchert, Y. Gao, J. Geiger, L. Giannone[4], U. Höfel, M. Hirsch, Z. Huang[5], J. Knauer, P. Kornejew, T. Kremeyer, M. Krychowiak, R. König, H.P. Laqua, R. Laube, D. Naujoks, N. Pablant[6], E. Pasch, F. Penzel[4] A von Stechow, H. Thomsen, Th. Wegner, G. Weir, V. Winters and the W7-X team

Max-Planck-Institut für Plasmaphysik, 17489 Greifswald, Germany
[1]University Carlos III of Madrid, 28911, Leganes, Spain
[2]Los Alamos National Laboratory, Los Alamos, USA
[3]Institute of Plasma Physics and Laser Microfusion (IPPLM), 01-497 Warsaw, Poland
[4]Max-Planck-Institut für Plasmaphysik, Garching, Germany
[5]Plasma Science and Fusion Center, MIT, Cambridge, MA 02139, USA
[6]Princeton Plasma Physics Laboratory, Princeton, NJ, US

Introduction. In the neoclassically optimized W7-X stellarator, particle and energy transport has so far been dominated by turbulent transport, especially in gas-fueled plasmas generated by ECRH, where the transport time for impurities is much shorter than predicted by neoclassical theory and the energy confinement time is somewhat below the ISS04 stellarator scaling [1-4]. In addition, the ion temperature T_i is usually limited to 1.5 keV, except in some special cases wherein this limitation is removed (cf. Fig. 10 [5]). During the normal experimental programs (which typically last ~10 s), no obvious accumulation of impurities has been observed so far. Therefore, the plasma radiation profiles are typically hollow with a peak at the plasma edge associated with intrinsic low-Z impurities (typically carbon and oxygen from the plasma facing components (PFC) at W7-X). Recently, plasma phases with prominent radiation from the inner plasma region have been revealed by bolometer tomography [6] in two long-pulse hydrogen discharges (up to ~50 s; ECRH power 1.2 MW in the initial phase and later halved), which were performed shortly after wall boronization during the first divertor operational phase. The radiation intensity there (at r/a~0.3-0.4) are comparable to that at the plasma edge (r/a≥0.8). Spectroscopic diagnostics show an increasing of high-Z impurity content (mainly Fe ions) and their accumulation in the plasma core. These discharges are among the exceptions mentioned above in Ref. [5]. In this work, we report the observations in detail and show for the first time the compatibility of high Z impurity accumulation with relatively high plasma performance in the studied ECR-heated W7-X plasmas. In addition, we are investigating the mechanisms that evolve higher plasma confinement (i.e., turbulence suppression) and trigger impurity accumulation - an effect of neoclassical impurity transport after turbulence transport has been suppressed.

Experimental descriptions. The studied discharges are XP20180808.5 and .7 (hereafter noted as XP5 and XP7, respectively). The magnetic configuration is 'high-iota' with a plasma minor radius a=0.5m (~2cm smaller than the mostly studied 'standard' configuration). During the discharges, gas refueling is alternately turned on and off. Fig. 1 shows the associated diagnostics, on the left for XP5 and on the right for XP7. From top to bottom, they are the heating power P_{ECRH}, the total radiated power loss P_{rad}, the line-averaged plasma density $\langle n_e \rangle$, the gas flow, the electron temperature $T_e(0)$ and $T_{e,edge}$ from channels 13 and 29 of the ECE diagnostic, $T_i(0)$ from XICS diagnostic, the plasma stored energy W_p measured with a compensated diamagnetic loop, the soft x-ray (SXR) signal from a bolometer channel covered with a 12-μm Be filter, and the H_α signal from divertor cameras (not available for XP7).

The time-slots chosen in Fig.1 are mainly for showing the transition phases interested, e.g. the built-up of Wp and simultaneously the enhancement of the SXR-level, which is marked by arrows (in black).

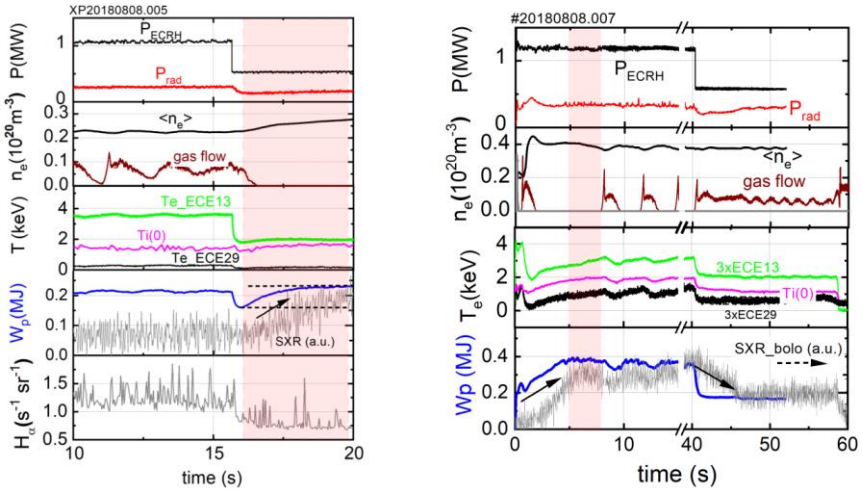

Fig.1 Time traces of the relevant diagnostics for XP5 (left) and XP7(right). From top to bottom: P_{ECRH}, P_{rad}, <n_e>, gas-flow, T_e from ch13 and ch29 of the ECE diagnostic, $T_i(0)$ from XICS, the plasma stored energy W_p, the soft-X ray and H_α signal (not available for XP7).

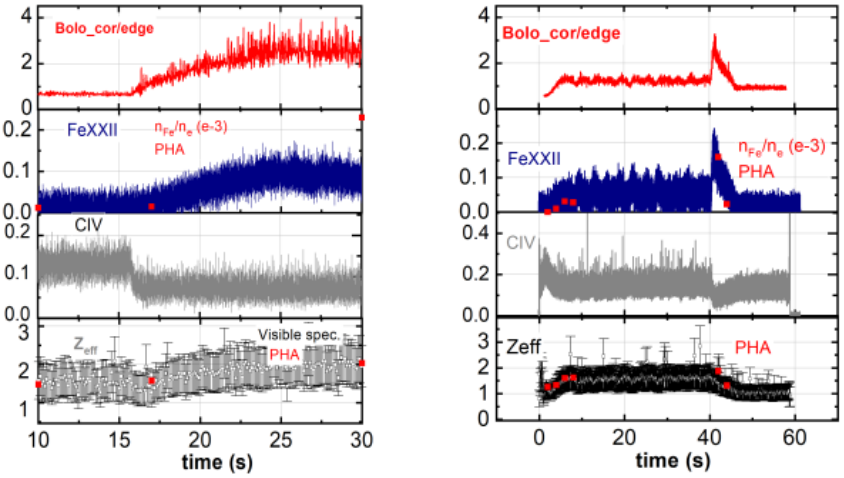

Fig. 2 Time traces of impurity-related diagnostics for XP5 in the left panels and XP7 in the right panels. From top to bottom: ratio of ch-core and -edge from bolometers (red line), PHA (red cubes), FeXXII and CIV from HEXOS, Z_{eff} from visible spectroscopy and estimated by PHA.

Our observations for XP5, in particular for the plasma phases after decreasing P_{ECRH} and then turning off the gas puff (t>16s), are 1) an increase in <n_e>, 2) a gradual increasing of $T_i(0)$ reaching 1.6 keV, 3) an increase in W_p accompanied by an increase in SXR emission. Besides, the $H\alpha$ value measured by a divertor camera decreases; distinct regular ILM's (island localized mode [12]) appear, indicating a transition to another phase. After a few seconds, the plasma stabilizes and reaches a higher performance (HP) regime where both W_p and $T_i(0)$ have higher values, although the P_{ECRH} is halved; this leads to an energy confinement time τ_E = 0.4s (0.2s in the normal phase NP) and a higher ratio of τ_E/τ_{ISS04} ~1 (0.7 in the NP phase). Here, τ_{ISS04} is the energy confinement time determined based on ISS04 scaling [7] $\tau_{ISS04} = 0.134a^{2.28}R^{0.64}P^{-0.61}n_e^{0.54}B^{0.84}\iota_{2/3}^{0.41}$, using a=0.5m, R=5.5m, B=2.39 T, ι=1.1, P=P_{ECRH} and n_e=<n_e> from the experiments. By contrast, in XP7 the transition to a HP phase occurs before the reduction of P_{ECRH}, and also after turning off of the gas puff at t=1.4s: 1) $T_e(0)$ and $T_{e,edge}$ increase obviously; 2) $T_i(0)$ approaches 2 keV, 3) similar to XP5, W_p and SXR emission increase simultaneously. A quasi-stationary HP phase with a value of τ_E/τ_{ISS04} ~1 is reached after a few seconds of transition time and lasts more than 35 seconds until the reduction of P_{ECRH}. In the later phase (t>40s; 0.6MW), the gas supply turns

on continuously, the value of τ_E/τ_{ISS04} degrades to ~0.6 and both W_p and SXR emission drop off with decay times of ~0.5s and ~6s, respectively, roughly corresponding to the time of energy and impurity confinement. During the HP phase, a slight decrease in W_p is observed when the gas puff is temporarily turned on, suggesting that this excessive gas supply causes a degradation in the energy confinement. This relationship can be seen in Fig. 3(a), which summarizes the gas-flow (in brawn), the calculated τ_E (in green) based on W_p, τ_{ISS04} (in black), and their ratio (in red). Moreover, the density profiles (measured by Thomson scattering) show a flattening effect due to gas puffing; a pure recycling neutral fuel leads to a more peaked profile with a steep gradient, as shown in Fig. 3(b). Comparing the profiles in the HP and NP phases of XP5 and XP7, the same conclusion is reached (More details will be presented elsewhere).

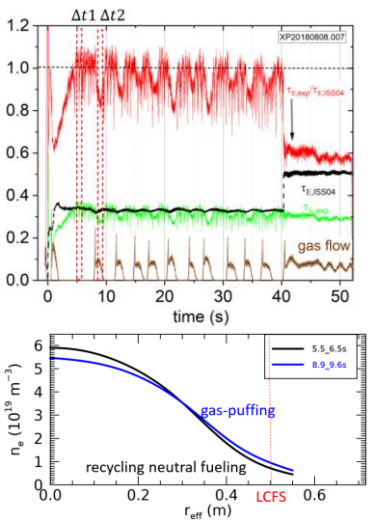

Fig. 3 (a) Demonstration of the impact of gas-fueling on the plasma confinement time in XP7: the ratio of τ_E/τ_{ISS04} in red, the $\tau_{E,ISS04}$ in black, the τ_E in green and the gas-flow in brown; (b) A comparison of the n_e-profiles for the two marked time-slots in (a) shows the flattening of the n_e-profile due to gas-puff (in blue).

Radiation profiles and impurity transport. The high SXR emissions in the HP-regime depicted in Fig. 1 originate from the deep, confined plasma region, as evidenced by the radiation profiles obtained with the bolometer tomography. They are shown in Fig.4. The 2D emission patterns and the poloidally averaged radial emission profiles for both HP and NP phases are shown in Fig.4 for comparisons. The prominent radiation intensity at r/a~0.3-0.4 for t=30s in XP5 and t=10s in XP7 indicate the existence of high-Z element emission. This is confirmed by spectroscopic measurements (HEXOS) and pulse height analysis (PHA); high-Z element such as Fe is detected in addition to the elements C, O, S and Cl. The maximum Fe ion concentrations of about 0.02% and <0.01% in the HP phases of XP5 and XP7 are determined by PHA system. The FeXXII emission from HEXOS increases continuously during the buildup of the HP phases, which is consistent with the SXR emission for both discharges as shown in Fig. 1(in grey). Additionally, an increase in the effective ion charge Z_{eff} (from 1.2 to 1.9) is obtained based on the visible bremsstrahlung measurements. All these are shown in Fig. 2, left for XP5 and right for XP7, respectively. Note that CIV emission decreases generally in the HP-phases or after

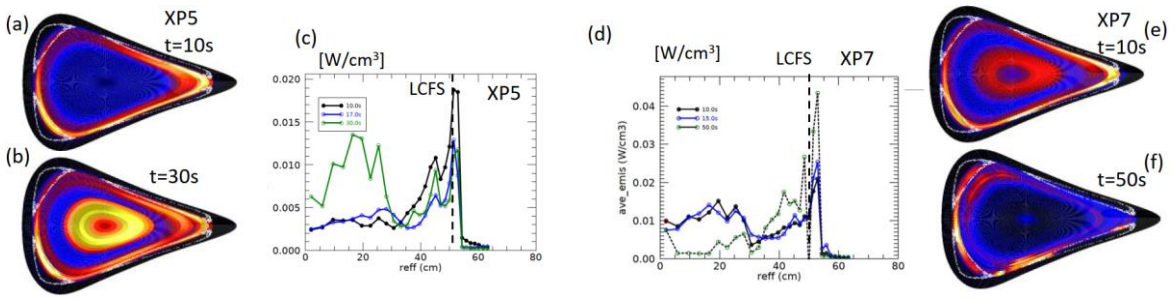

Fig. 4 The 2D emission patterns obtained by bolometer tomography and the poloidally averaged radial emission profiles for selected time points for XP5 in (a-c) and for XP7 in (d-f), respectively.

reduction of the P_{ECRH}.

Simulations of Fe ion emission using STRAHL[8] code under the current plasma conditions were performed for t=20 s in the HP phase of XP5. A diffusion coefficient of D=0.1m^2/s and an inward convective V for the outer confinement region (r/a>0.5) with $V(r/a=1)$ = -0.1 m/s and an outward one in the inner region are essential to obtain a comparable emission profile as shown in Fig. 4 (c). The latter is comparable to the neo-classical theroy predicted one, V_{neo}, that obtained with DKES [9] simulations while the D-value is still obviouly higher than D_{neo}~0.01m^2/s.

Discussions and Summary. Higher performance plasma phases ($T_i(0)$ >1.5 keV; τ_E/τ_{ISS04} ~1) accompanied by high Z element accumulation in the inner plasma region have been observed in low power hydrogen plasmas (at 0.6 MW in XP5 and 1.2 MW in XP7, respectively). Further analyses performed show that a common condition for the occurrence of this scenario is the peak of the plasma density profile with a steep gradient and a low edge plasma density (<1.0 10^{19} m^{-3}) obtained by pure recycling neutral fueling from the divertors. Such gradient steeping causes usually a reduction of turbulence transport in W7-X[10, 11] (similar to the pellet injection experiments). However, direct measurements of the turbulence level were not made during these experiments. The electrostatic instabilities on the ion scale analyzed by linear gyro kinetic simulations confirm a low growth rate in the HP phase for XP5, while that in XP7 is comparable to that in the NP phase, which requires further investigations. We conclude that 1) the observed enrichment of impurities in the inner plasma region (e.g., in XP5) is a neoclassical effect due to the suppression of turbulence by increasing the density gradient; 2) the source of the high-Z elements could be from active impurity injection experiments (e.g., laser blow-off), which are deposited on the PFCs and are released under suitable conditions upon entering the confined plasma region. Further investigations in other magnetic configurations will be conducted in the upcoming experimental campaign.

Acknowledgment

This work has been carried out within the framework of the EUROfusion Consortium, funded by the European Union via the Euratom Research and Training Programme (Grant Agreement No 101052200 — EUROfusion). Views and opinions expressed are however those of the author(s) only and do not necessarily reflect those of the European Union or the European Commission. Neither the European Union nor the European Commission can be held responsible for them.

References:

[1] Beidler, C., et al., Nature, 2021. **596**(7871): p. 221-226.
[2] Geiger, B., et al., Nuclear Fusion, 2019. **59**(4): p. 046009.
[3] Langenberg, A., et al., Physics of Plasmas, 2020. **27**(5): p. 052510.
[4] Fuchert, G., et al., Nuclear Fusion, 2020. **60**(3): p. 036020.
[5] Beurskens, M.N., et al., Nuclear Fusion, 2021.
[6] Zhang, D., et al., Nuclear Fusion, 2021. **61: p.**116043
[7] Yamada, H., et al., Nuclear Fusion, 2005. **45**(12): p. 1684.
[8] Dux, R., *STRAHL user manual.* 2006; K. Behringer, JET-R(87)08
[9] Maaßberg, H., C. Beidler, and Y. Turkin, Physics of Plasmas, 2009. **16**(7): p. 072504.
[10] Alcusón, J., et al., Plasma Physics and Controlled Fusion, 2020. **62**(3): p. 035005.
[11] Stechow, A.v., et al., *Suppression of core turbulence by profile shaping in Wendelstein 7-X.* arXiv preprint arXiv:2010.02160, 2020.
[12] Wurden, G. et al., this conference, P1b.118